Journal of Mines, Metals and Fuels, *71(10): 1501-1510; 2023. DOI: 10.18311/jmmf/2023/ 35790*

Print ISSN : 0022-2755

Journal of Mines, Metals and Fuels

Contents available at: *www.informaticsjournals.com/index.php/jmmf*

Effect of Forchheimer on Hydromagnetic Flow Inspired by Chemical Reaction Over an Accelerating Surface

M. Girinath Reddy[1]*, P. A. Dinesh[1], A. Sreevallabha Reddy[1] and Uma Raju[2]

[1]Department of Mathematics, M. S. Ramaiah Institute of Technology (Affiliated to VTU), Bangalore - 560054, Karnataka, India; girinath@msrit.edu, dineshdpa@msrit.edu, sreesiri@gmail.com

[2]Department of Mathematics, C. M. R Institute of Technology (Affiliated to VTU), Bangalore - 560037, Karnataka, India; uma.v@cmrit.ac.in

Abstract

This study investigates the effects of Forchheimer and Lorentz on paired heat and mass transfer by MHD twinned convective flow of a Newtonian fluid with the chemical reaction effect through porous media over an accelerating surface. The governing equations of the physical model are the non-linear coupled PDEs, which are converted to a system of coupled non-linear ODEs with a suitable similarity transformation. By implementing the Shooting technique, the computations are drawn numerically for the distributions of velocity, thermal variations and species changes for distinct dimensionless parameters such as Hartmann number, buoyancy parameters, porous parameter, local inertial parameter, Prandtl number, viscosity parameter, Eckert number and chemical reaction parameter etc. Also, the numerical computations of flow velocity, temperature and species concentration are illustrated graphically for the important physical parameters.

Keywords: *Forchheimer Effect, MHD, Porous Medium, Chemical Reaction, Accelerating Surface.*

1.0 Introduction

In recent years, many authors devoted to study the combined application of mixed MHD convective flow through porous media. In hydro magnetic fluid flows, the effect of MHD on boundary layer problems through porous media has been seen in many practical applications such as oil extraction, thermal insulations and geothermal energy recovery. Also, the hydro magnetic fluid flows under the chemical reaction plays an important role in metal industries, in the field of mining and emphasizing on our basic needs like oils and fuels. In the above-mentioned applications, several authors come across fluid properties like permeability, viscosity, porosity, diffusivity and conductivity considered as constants. Furthermore, the research scholars have extended the work of the above physical models by considering fluid properties as constants and with the accelerating surface. The first and foremost research work related to the above industrial applications for a fluid flow leading by a continuous solid flat surface were studied by Sakiadis[1]. Later, Vleggaar[2] explained the boundary-layer laminar flow on a continuous moving surface. The effect of mass transfer on fluid flow over a past moving vertical plate was investigated by Soundalgekar[3]. For many physical systems, it is understood that the variable fluid properties fluid viscosity varies concerning temperature i.e. the enhancement of temperature leads to a rise in the fluid viscosity so to estimate more accurately the flow rate and heat transfer rate, it is very much required to consider viscosity variation into an account. Lai and Kulacki[4] examined the convective heat transfer flow via a porous vertical surface with variable viscosity. Mass transfer and free convective flow through a saturated porous medium

**Author for correspondence*

with heat source, unchanged suction velocity and heat flux over the vertical infinite flat surface was analyzed by Acharya *et al.*[5].

Chandrasekhar and Namboodiri[6] investigated the effect of variable permeability on velocity and temperature distributions through a porous medium. Further, Veera Krishna *et al.*[7-9] scrutinized the responses of free or mixed convective flow and mass transfer of MHD secondary grade fluid along a constant/accelerating /stretching plate via a porous medium experienced by various effects. Later, the impact of nonlinear thermophoresis on both natural and forced convective flow surrounded by sphere surface inspired by variable conductivity and viscosity varying with temperature was studied numerically by the scholars[10,11]. The compound effect of a chemical reaction and magnetic field through a porous medium play a very important role in recent engineering and chemical applications for instance, in the transport phenomena changes by the newly generated concentration species due to chemical reaction effect on ambient fluid and which results on the quality of the final product. Mallikarjuna *et al.*[12] have investigated chemical reactions and variable porosity effects on double-diffusive MHD convective flow along a rotating vertical cone. Later, several authors[13,14] made an attempt to investigate the catalytic exothermic chemical phenomenon of free forced convection flow over a curved surface.

Reddy *et al.*[15,16] examined the combined effects of temperature and concentration called double-diffusive convection with an inclusion of the external heat source as internal heat generation under the effect of variable viscosity and permeability for cross diffusion effects such as Soret and Dufour over an accelerating surface. Basavaraj *et al.*[17] carried a work on nonlinear mixed convective and uniform magnetic field over a vertical plate of oscillatory flow through a porous medium. Muhammad *et al.*[18] developed the Forchheimer model to demonstrate the characteristics of flow and heat transfer of mixed convection flow by incorporating entropy generation and activated energy through a stretched curved sheet. Girinath Reddy *et al.*[19] gave the numerical approach of MHD over an accelerating surface with effects of Soret and Dufour on concentric heat flow. Recently, to understand the MHD mixed heat transfer on Couette flow under dusty viscoelastic property through irregular channel numerically for the dimensional parameters of Forchheimer, Soret and Dufour studied by Dinesh *et al.*[20]. Further, the physical behavior of Forchheimer model of natural and forced convective flow under the impact of Soret and Dufour effects in the presence of magnetic field via a heated plate fixed vertically explained by Nalinakshi *et al.*[21]. Furthermore, the effects of magnetic field on mixed convection over a vertical heated plate with variable fluid properties through a porous medium with and without experience of chemical reaction noticed by the authors[22,23].

As per our knowledge, the researchers have not made an attempt so far to analyze the combined effects of Lorentz and Forchheimer on the MHD mixed convection heat and mass transfer flow in the presence of chemical reaction over an accelerating plate through a porous medium with variable fluid properties of the media which leads the novelty of this paper.

2.0 Formulation of the Problem

A double-diffusive and combined free-forced (mixed) convective flow of an incompressible, laminar, two-dimensional, steady, electrically conducting and viscous fluid over an accelerating vertical plate through saturated porous medium with variable viscosity, variable porosity and permeability under the magnetic field B_0 applied uniformly along the vertical direction is considered. Here plate moves along the x-axis and which is orthogonal to y-axis. Assume that the vertical plate is non-electrically conducted so that the effect of magnetic Reynolds number is very small. The constant injection velocity $v = v_w$ and the linear velocity $u = bx$ are maintained along with

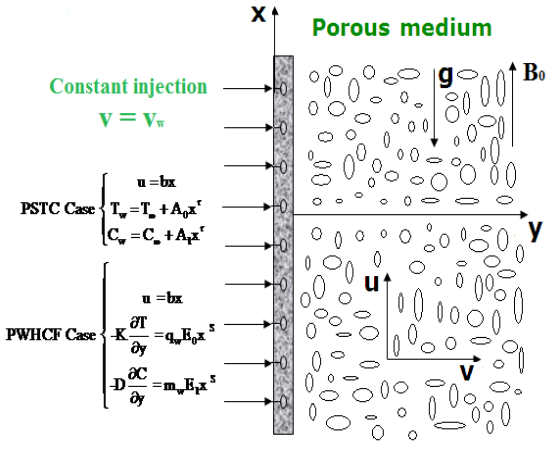

Figure 1. Physical Model.

coordinate axes respectively. The geometry of the physical model of the fluid flow is visualized in Figure 1.

The mathematical governing equations are drawn by incorporating the external or internal effects caused due to heat and mass transfer of the fluid. The assumptions are made along with the Boussinesq approximation for the above flow geometry of the fluid (i) Lorentz force and Forchheimer effect are applied; (ii) the viscosity is varying inversely with respect to a linear function of temperature, i.e. $\frac{1}{\mu}=\frac{1}{\mu_\infty}\left[1+\gamma(T-T_\infty)\right]$ or $\frac{1}{\mu}=\alpha(T-T_v)$ (see Lai *et al.*[4]), where $\alpha=\frac{\gamma}{\mu_\infty}$, $T_v=T_\infty-\frac{1}{\gamma}$ are the constants but varies with thermal property of the fluid γ; (iii) chemical reaction of l^{th} order with homogeneity is taking in to account.

$$u_x+u_y=0, \tag{1}$$

$$uu_x+vu_y=\frac{1}{\rho}\left(\mu u_y\right)_y+g\beta_T\left(T-T_\infty\right)-g\beta_C\left(C-C_\infty\right)-\frac{\xi(y)\bar{\mu}u}{\rho\kappa(y)}-\frac{\sigma_m B_0^2\xi(y)u}{\rho}-\frac{\xi^2(y)C_b u^2}{\sqrt{\kappa(y)}}, \tag{2}$$

$$uT_x+vT_y=\frac{k}{\rho C_p}T_{yy}+\frac{\mu}{\rho C_p}\left(u_y\right)^2+\frac{\bar{\mu}\xi^2(y)u^2}{\rho C_p\kappa(y)}-\frac{\sigma_m B_0^2\xi^2(y)u^2}{\rho C_p}, \tag{3}$$

$$uC_x+vC_y=D_mC_{yy}-K_R\left(C-C_\infty\right)^l, \tag{4}$$

where u *and* v are the velocity field components, all the existing physical quantities in Eqs. (1) - (4) are mentioned under nomenclature section. The expressions of permeability $\kappa(y)$ and porosity $\xi(y)$ are the functions of vertical coordinate y, which are defined by Chandrasekhara and Namboodiri[6].

$$\kappa(y)=k_0(1+de^{-y}) \text{ and } \xi(y)=\varepsilon_0(1+d^*e^{-y}), \tag{5}$$

where $d=3.0$ and $d^*=1.5$ are the fixed values of variable permeability and porosity respectively. k_0 & ε_0 are respectively permeability and porosity at the edge of the boundary.

We have considered the two different special cases, Prescribed Surface Temperature (PST) and Wall Heat Flux (WHF) to study the flow characteristics of the physical model for different boundaries.

2.1 Prescribed Surface Temperature (PST)

Here, we assumed the temperature T_w of the accelerating vertical plate and concentration of the accelerating wall C_w at every point of the boundary surface are respectively in the form of $T_w=T_\infty+A_0x^r$ and $C_w=C_\infty+A_1x^r$. As per the considered geometry of the physical system the boundary conditions are

$$u=bx,\ v=v_w,\ T_w=T_\infty+A_0x^r,\ C_w=C_\infty+A_1x^r \quad \text{for } y=0, \tag{6}$$

$$u(\infty)=0,\quad T(\infty)=T_\infty,\quad C(\infty)=C_\infty, \tag{7}$$

where b is accelerating plate's stretching rate, r is temperature parameter and A_0 & A_1 are the arbitrary constants. The Equations (10) - (12) are obtained from Equations (2) - (4) using similarity variable and the non-dimensional quantities given by Acharya *et al.*[5] along with Equation (9).

$$\eta=\left(\frac{b}{\upsilon}\right)^{\frac{1}{2}}y,\quad \psi=(\upsilon b)^{\frac{1}{2}}x\,f(\eta),\quad \theta(\eta)=\frac{T-T_\infty}{T_w-T_\infty},\quad H(\eta)=\frac{C-C_\infty}{C_w-C_\infty}, \tag{8}$$

where the velocity components are defined as

$u=\frac{\partial\psi}{\partial y}$ *and* $v=-\frac{\partial\psi}{\partial x}$ and which are

$$u=bxf'(\eta),\quad v=-(b\upsilon)^{\frac{1}{2}}f(\eta), \tag{9}$$

$$f'''-\left(\frac{1}{\theta-\theta_r}\right)\theta' f''-\left(\frac{\theta}{\theta_r}-1\right)\left(ff''-f'^2\right)+\alpha^*\varepsilon_0\sigma\left(\frac{1+d^*e^{-\eta}}{1+de^{-\eta}}\right)\left(\frac{\theta}{\theta_r}-1\right)f'+\beta^*\left[\frac{\left(1+d^*e^{-\eta}\right)^2}{\left(1+de^{-\eta}\right)^{1/2}}\right]$$

$$\left(\frac{\theta}{\theta_r}-1\right)f'^2+M^2\varepsilon_0\left(1+d^*e^{-\eta}\right)\left(\frac{\theta}{\theta_r}-1\right)f'=\left(\frac{\theta}{\theta_r}-1\right)(Gs\,\theta-Gc\,H), \tag{10}$$

$$\theta''+\Pr f\,\theta'-r\Pr f'\theta=-E\Pr f''^2-E\,\sigma\Pr\varepsilon_0^2\left[\frac{(1+d^*e^{-\eta})^2}{1+de^{-\eta}}\right]f'^2+$$

$$EM^2\Pr\varepsilon_0^2(1+d^*e^{-\eta})^2f'^2, \tag{11}$$

$$H''+Sc\,f\,H'-r\,Sc\,f'H=K_rH^l, \tag{12}$$

The transformed boundary conditions are

$$f(0)=-\frac{v_w}{(b\upsilon)^{\frac{1}{2}}}=-m,\quad f'(0)=1,\quad \theta(0)=1,\quad H(0)=1, \tag{13}$$

$$f'(\infty)=0,\quad \theta(\infty)=0,\quad H(\infty)=0, \tag{14}$$

2.2 Prescribed Wall Heat Flux (PWHF)

In this case, both the temperature and concentration changes with respect to y-coordinate i.e. $-k\frac{\partial T}{\partial y}=q_w E_0 x^s$ and $-D\frac{\partial C}{\partial y}=m_w E_1 x^s$, the associated boundary conditions are

$$u=bx,\ v=v_w,\ -k\frac{\partial T}{\partial y}=q_w E_0 x^s,\ -D\frac{\partial C}{\partial y}=m_w E_1 x^s,$$

for $y=0,$ (15)

$$u(\infty)=0,\quad T(\infty)=T_\infty,\quad C(\infty)=C_\infty,\qquad (16)$$

Where E_0 & E_1 are the arbitrary constants and s is the thermal flux parameter. Similarly, the Equations (18)-(20) are obtained from the Equations (2) - (4) with the use of the similarity variable and the non-dimensional quantities given by Acharya *et al.*[5] along with Equation (9).

$$\eta=\left(\frac{b}{\upsilon}\right)^{\frac{1}{2}}y,\quad \psi=(\upsilon b)^{\frac{1}{2}}x f(\eta),\quad T-T_\infty=\frac{E_0 x^s}{k}\left(\frac{\upsilon}{a}\right)^{\frac{1}{2}}g(\eta),\quad C-C_\infty=\frac{E_1 x^s}{D}\left(\frac{\upsilon}{a}\right)^{\frac{1}{2}}h(\eta),\qquad (17)$$

$$f''''-\left(\frac{1}{g-g_r}\right)g'f'''-\left(\frac{g}{g_r}-1\right)\left(ff'''-f'^2\right)+\alpha^*\varepsilon_0\sigma\left(\frac{1+d^*e^{-\eta}}{1+de^{-\eta}}\right)\left(\frac{g}{g_r}-1\right)f'+$$

$$\beta^*\left[\frac{\left(1+d^*e^{-\eta}\right)^2}{\left(1+de^{-\eta}\right)^{1/2}}\right]\left(\frac{g}{g_r}-1\right)f'^2+M^2\varepsilon_0\left(1+d^*e^{-\eta}\right)\left(\frac{g}{g_r}-1\right)f'=$$

$$\left(\frac{g}{g_r}-1\right)(Gs\,g-Gc\,h),\qquad (18)$$

$$g''+\Pr f\,g'-s\Pr f'g=-E\Pr f''^2-E\,\sigma\Pr\varepsilon_0^2\left[\frac{(1+d^*e^{-\eta})^2}{1+de^{-\eta}}\right]f'^2+$$

$$-EM^2\Pr\varepsilon_0^2(1+d^*e^{-\eta})^2f'^2,\qquad (19)$$

$$h''+Sc\,f\,h'-s\,Sc\,f'h=K_r h^l,\qquad (20)$$

The transformed boundary conditions are

$$f(0)=-\frac{v_w}{(b\upsilon)^{\frac{1}{2}}}=-m,\quad f'(0)=1,\quad \theta(0)=1,\quad H(0)=1,\qquad (21)$$

$$f'(\infty)=0,\quad g(\infty)=0,\quad h(\infty)=0.\qquad (22)$$

All the involved dimensionless quantities are presented under the nomenclature section.

3.0 Conclusions

The drawn numerical computations are shows the variations of velocity, temperature differences and solutal changes for different non-dimensional parameters like Hartmann number, local inertial parameter, chemical reaction parameter, Eckert number, viscosity parameter, porous parameter, Prandtl number, temperature and mass buoyancy parameters etc. of physical problem are explained in the Figures 2-18. In all the results, except the values varying as shown in the respective figures, we fixed the values of dimensionless parameters as $\Pr=0.7$, $E=0.6$, $M=0.5$, $Gs=0.1$, $Gc=0.1$, $\theta_r=3.0$, $g_r=3.0$ $Sc=0.6$, $r=1$, $s=1$, $m=-0.2$, $\varepsilon_0=0.1$, $\sigma=0.5$, $\alpha^*=0.1$, 0.5, $K_r=0.2$, $l=2$.

The effect of the uniform magnetic field with the Joule effect plays a major role in controlling the velocity profile of the fluid seen in Figure 2. Here, the velocity of the flow decreases with an increase of Hartmann number M, which is due to the effect of Lorentz force. But, the Figures 3 and 4 respectively illustrated a reverse trend of temperature and concentration profiles with higher values of Hartmann number M. The enhancement magnetic fluid accelerates the flow temperature and which leads the heat convection rate will reduce in the fluid flow. Similarly, we can also observe that for higher values of magnetic field parameter the dimensionless concentration increases.

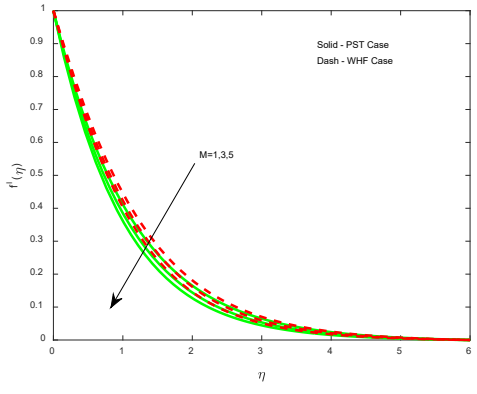

Figure 2. Result of M on flow filed

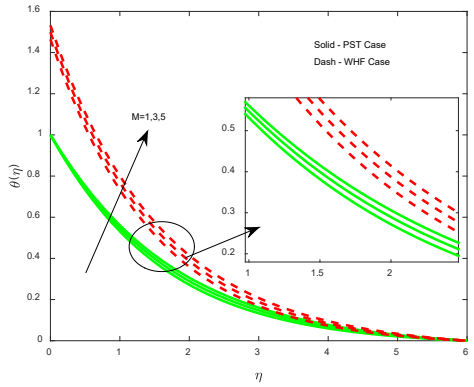

Figure 3. Result of M on energy filed.

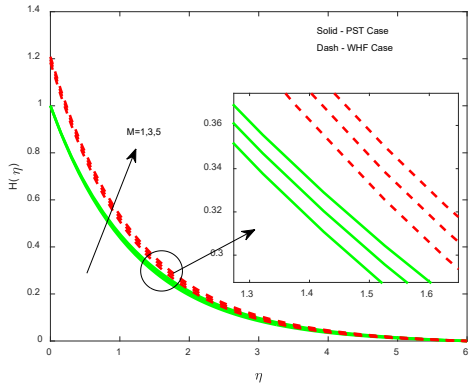

Figure 4. Result of M on concentration filed.

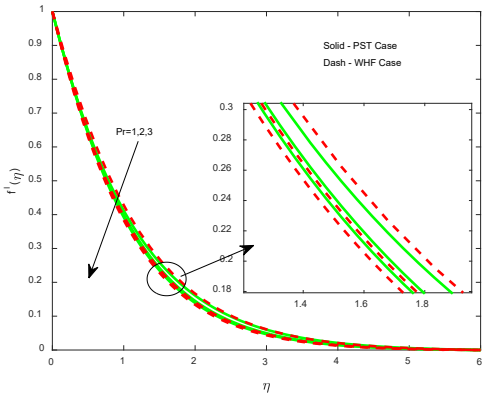

Figure 5. Result of Pr on flow filed.

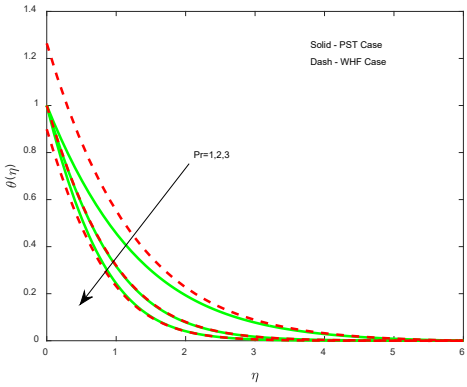

Figure 6. Result of Pr on energy filed.

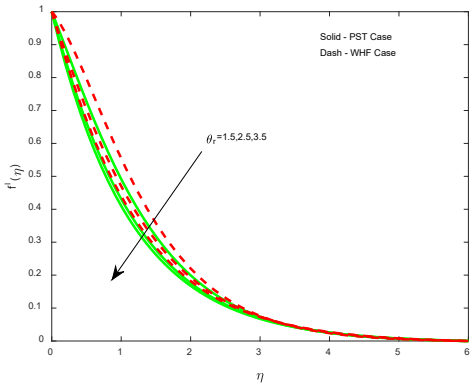

Figure 7. Result of θ_r on flow filed.

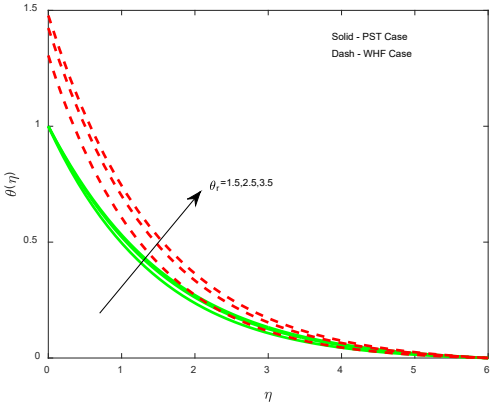

Figure 8. Result of θ_r on energy filed.

The variations of Prandtl number Pr in terms of velocity and temperature shown in Figures 5 and 6 respectively. The variations of the Prandtl number Pr depends on thermal diffusivity or viscosity i.e. the Prandtl number Pr increases with more viscosity of the fluid or less thermal diffusivity. The flow velocity and temperature of the fluid decrease with an enhancement of fluid viscosity. The effect of viscosity parameter θ_r on velocity,

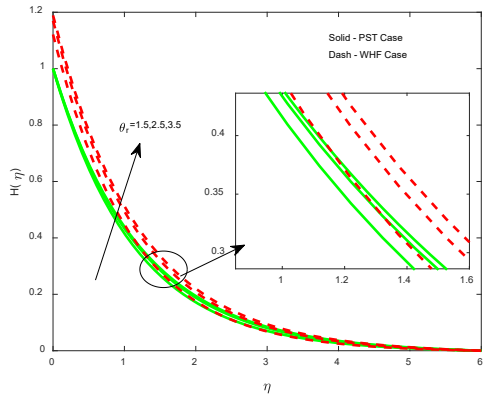

Figure 9. Result of θ_r on concentration filed.

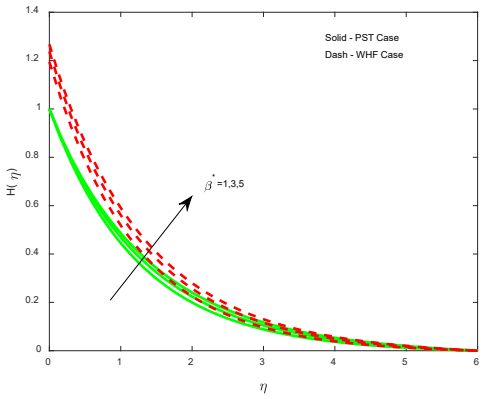

Figure 12. Result of β^* on concentration filed.

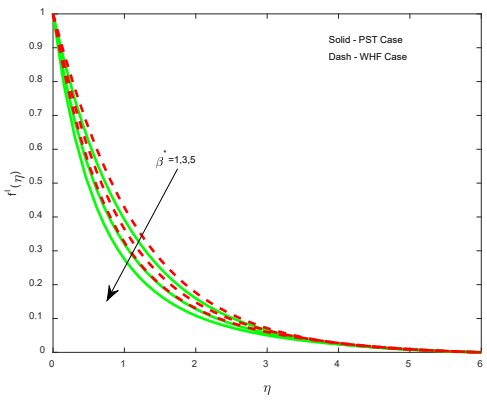

Figure 10. Result of β^* on flow filed.

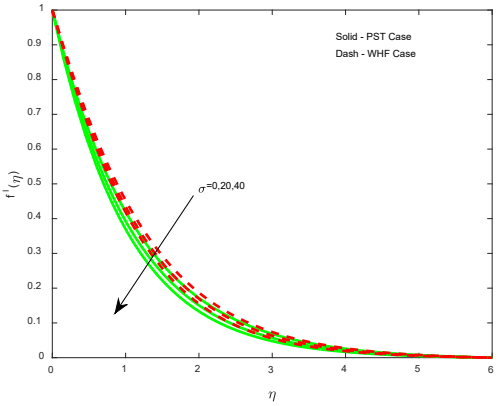

Figure 13. Result of σ on flow filed.

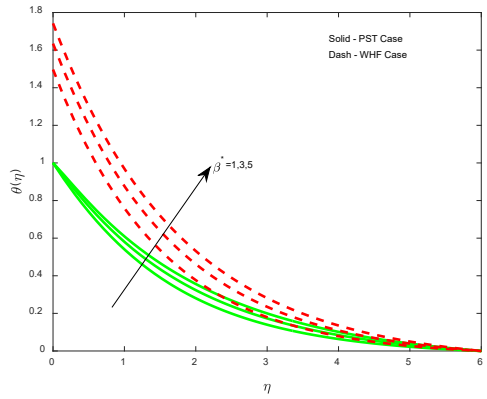

Figure 11. Result of β^* on energy filed.

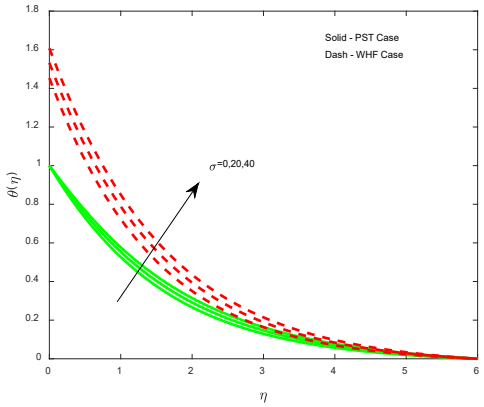

Figure 14. Result of σ on energy filed.

temperature and concentration profiles are shown in Figures 7-9 respectively. Velocity distribution reduces for an enhancement of viscosity parameter θ_r, which can be detected from Figure 7. But the hike of viscosity

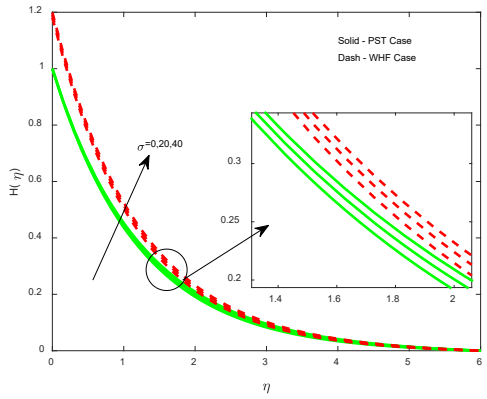

Figure 15. Result of σ on concentration filed.

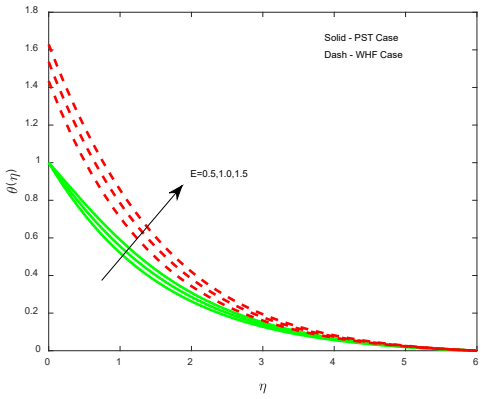

Figure 17. Result of E on energy filed.

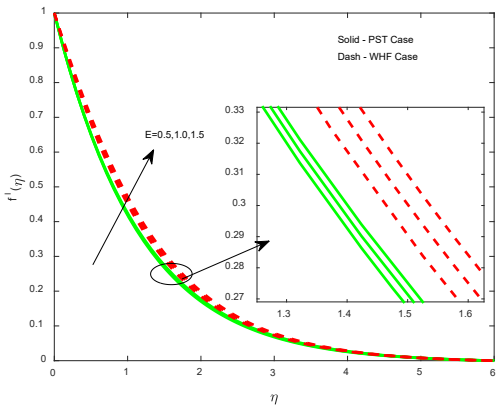

Figure 16. Result of E on flow filed.

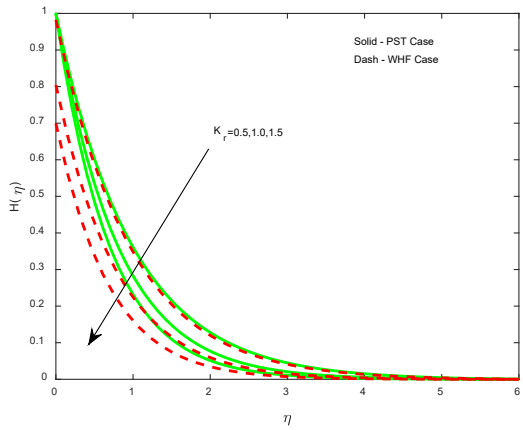

Figure 18. Result of K_r on concentration filed.

parameter θ_r boosted the temperature and concentration distributions, which are illustrated in Figures 8 and 9 respectively.

The numerical computations for the effect of different values of second-order resistance β^*(local inertial parameter) on dimensionless distributions of momentum, thermal and concentration are depicted in Figures 10-12. The enhancement of inertial parameter β^* is with the less of permeability or hike of porosity of the porous medium, which yields the reduction of the flow velocity of the fluid in both the cases WHF and PST, which is due to the fluid flow with high porosity of the porous medium slows down the flow velocity, presented in Figure 10. Also, we can observe that for higher values of β^* the dimensionless temperature and concentration profiles rapidly increases, which can be gleaned from Figures 11 and 12 respectively. This indicates that the case of WHF is more predominant than PST case.

The porous parameter σincreases for enhancement of viscosity or decrement of stretching rate or lower permeability of the porous medium, which decelerates the flow velocity of the fluid as shown in Figure 13. But we can observe the opposite trend from Figures 14 and 15. i.e. with the involvement of enhancement of the effect of viscosity or with the lesser permeability of the porous medium results in the reduction of the movement of the fluid and will intern increases the profile of the temperature and acceleration of the concentration in the fluid motion both in PST and WHF cases. Also, it is observed that the effect of a porous parameter is more in the temperature profile compare to velocity and concentration profiles.

Figures 16 and 17 display the variations of Eckert number E over the velocity and temperature profiles respectively, which contributes to understanding the Ohmic effect. With an enhancement of Eckert number E, the non-dimensional velocity and temperature

distributions overshoots. In the present work, it is noticed that the concentration profile is not affected by the Eckert number. Figure 18 indicates the behavior of the chemical reaction parameter K_r on the species layer. It is noticed that, in both the cases of PST and WHF the fluid concentration gradients reduce for higher values of K_r and higher order of chemical reaction. Due to the isosolutal and impermeable boundary conditions maintained at the accelerating plate and far away from the plate the percentage of decrement is predominant in WHF compared to that of PST case for concentration profile.

In this study, the flow characteristics of velocity, mass and heat transfer of the fluid are explained graphically for the distinct physical parameters. The important conclusions are listed below.

- The solutal and thermal distributions are boosted with the hike of M but it retards the flow velocity due to the drag effect from the magnetic field.
- More reduction in flow velocity with growth of β^* whereas opposite trend is seen with thermal and concentration boundaries.
- Dimensionless velocity is retarding but solutal and thermal boundaries are rising with greater θ_r and σ
- Increase of K_r minimizes the dimensionless concentration.
- Flow and thermal fields are slowed down with higher Pr but the reversal characteristic is detected with the strength of E.

4.0 Acknowledgements

The author(s) are sincerely thankful to the Research Centre, M. S. Ramaiah Institute of Technology for constant encouragement and generous support.

5.0 References

1. Sakiadis BC. Boundary-layer behavior on continuous solid surface: The boundary layer on a continuous flat surface. *AIChE J.* 1961; 7:221–225.
2. Vleggaar J. Laminar boundary-layer behaviour on continuous accelerating surface. *Chem. Engg. Sci.* 1977; 32:1517–1525.
3. Soundalgekar VM. Effects of mass transfer on flow past a uniformly accelerated vertical plate. *Lett. Heat Mass Transfer*. 1982; 9:65-72.
4. Lai FC and Kulacki FA. Effects of variable viscosity on convective heat transfer along a vertical surface in a saturated porous medium. *Int. J. Heat Mass Transfer* 1990; 33:1028.
5. Acharya M, Singh LP and Dash GC. Heat and mass transfer over an accelerating surface with heat source in presence of suction and blowing. *Int. J. Eng. Sci.* 1999; 37:189–211.
6. Chandrasekhara BC and Namboodiri PMS. Influence of variable permeability on combined vertical surfaces in porous medium. *International Journal of Heat Mass Transfer.* 1985; 28: 199-206.
7. Veera Krishna M, Gangadhara Reddy M and Chamkha AJ. Heat and Mass Transfer on MHD free convective flow over an infinite non-conducting vertical flat porous plate. *Int. J. Fluid Mech. Res.* 2019; 46(1):1-25.
8. Krishna MV, Jyothi K and Chamkha AJ. Heat and mass transfer on MHD flow of second-grade fluid through porous medium over a semi-infinite vertical stretching sheet. *J. Porous Media.* 2020; 23(8):751–765.
9. Veera Krishna M, Ameer Ahamad N and Chamkha AJ. Hall and ion slip effects on unsteady MHD free convective rotating flow through a saturated porous medium over an exponential accelerated plate. *Alexandria Eng. J.* 2020; 59:565-577.
10. Abbas A and Muhmmad A. Combined effects of variable viscosity and thermophoretic transportation on mixed convection flow around the surface of a sphere. *Therm. Sci.* 2020; 24(6):4089-4101.
11. Muhammad A. Numerical simulation of the combined effects of thermophoretic motion and variable thermal conductivity on free convection heat transfer. *AIP Advances* 2020; 10(8): 1-8(085005).
12. Mallikarjuna B, Rashad AM, Ali Chamkha J and Hariprasad Raju S. Chemical reaction effects on MHD convective heat and mass transfer flow past a rotating vertical cone embedded in a variable porosity regime. *Afr. Mat.* 2016; 27:645–665.
13. Ashraf M, Ahmad U and Chamkha AJ. Computational analysis of natural convection flow driven along curved surface in the presence of exothermic catalytic chemical reaction. *Comput. Therm. Sci.* 2019; 11:339–351.
14. Ahmad U, Ashraf M and Abbas A. Mixed convection flow along a curved surface in the presence of exothermic catalytic chemical reaction. *Sci. Rep.* 2021; 11:12907.
15. Girinath Reddy M, Dinesh PA and Sandeep N. Effects of variable viscosity and porosity of fluid, Soret and Dufour mixed double diffusive convective flow over an acceler-

ating surface. *IOP Conf. Series: Materials Science and Engineering.* 2017; 263: 1-13.
16. Girinath Reddy M and Dinesh PA. Double diffusive convection and internal heat generation with Soret and Dufour effects over an accelerating surface with variable viscosity and permeability. *Advances in Physics Theories and Applications.* 2018; 69, 7-25.
17. Basavaraj MS, Girinath Reddy M, Aruna AS, Dinesh PA. A nonlinear mixed convective oscillatory flow over a semi-infinite vertical plate through porous medium under uniform magnetic field. *International Journal of Advanced Research.* 2020; 8(6):308-321.
18. Muhammad R, Khan MI, Jameel M and Khan NB. Fully developed Darcy–Forchheimer mixed convective flow over a curved surface with activation energy and entropy generation. *Comput. Methods Programs Biomed.* 2020; 188:105298.
19. Girinath Reddy M, Dinesh PA, Basavaraj MS and Uma M. Numerical study of thermal-diffusion and diffusion-thermo effects on mixed convective flow and mass transfer in the presence of MHD over an accelerating surface. *Biointerface Research in Applied Chemistry.* 2021; 11(4):11487-11498.
20. Dinesh PA, Uma M, Girinath Reddy M and Sreevallabha Reddy A. Combined effects of Forchheimer, Soret and Dufour on MHD mixed convective dusty visco-elastic Couette flow in an irregular channel. *Journal of Multidiscipline in Modelling and Structures.* 2021; 17(1):49-64.
21. Nalinakshi N and Dinesh PA. Thermo-diffusion and diffusion-thermo effects for a Forchheimer model with MHD over a vertical heated plate. *Advances in Fluid Dynamics(LNME).* 2021; 343-361.
22. Suresh Babu R, Rushi Kumar B and Dinesh PA. Effects of variable fluid properties on a double diffusive mixed convection viscous fluid over a semi-infinite vertical surface in a sparsely packed medium. *Frontiers in Heat and Mass Transfer.* 2018; 10(3):1-9.
23. Girinath Reddy M, Dinesh PA, Basavaraj MS and Aruna AS. Effects of variable fluid properties on double diffusive mixed convection with chemical reaction over an Accelerating Surface. *Biointerface Research in Applied Chemistry.* 2022; 12(4):5161-5173.

Nomenclature

Magnetic number : $M = \sqrt{\frac{\sigma_m B_0^{\,2} L}{\rho U_0}}$	Local temperature Grashof number : $Gr_t = \frac{g\beta(T_w - T_\infty)x^3}{\upsilon_\infty^{\,2}}$
Prandtl number : $\mathrm{Pr} = \frac{\rho \upsilon_\infty C_p}{k}$	Local mass Grashof number : $Gr_m = \frac{g\beta^*(C_w - C_\infty)x^3}{\upsilon_\infty^{\,2}}$
Eckert number : $E = \frac{b^2 x^2}{C_p(T_w - T_\infty)}$	Chemical reaction parameter : $K_r = \frac{K_R\left(C_w - C_\infty\right)^{l-1}\upsilon}{bD_m}$
Schmidt number : $Sc = \frac{\upsilon_\infty}{D_m}$	Viscosity parameter for PST : $\theta_r = \frac{T_r - T_\infty}{T_w - T_\infty} = -\frac{1}{\gamma(T_w - T_\infty)}$

Reynolds number : $Re = \frac{u_0 x}{\upsilon}$	Viscosity parameter for WHF : $g_r = \frac{T_r - T_\infty}{T_w - T_\infty} = -\frac{1}{\gamma(T_w - T_\infty)}$
Ratio of viscosities : $\alpha^* = \frac{\mu}{\bar{\mu}}$	Mass buoyancy parameter : $Gc = \frac{Gr_m}{\mathrm{Re}^2}$
Porous parameter : $\sigma = \frac{\upsilon}{bk_0}$	Temperature buoyancy parameter : $Gs = \frac{Gr_t}{\mathrm{Re}^2}$
Constant injection : $V_w = m(b\nu)^{\frac{1}{2}}$	Local inertial parameter : $\beta^* = \frac{c_b \varepsilon_0^2 x}{k_0^{\frac{1}{2}}}$
C_p:specific heat	B_0:uniform transverse magnetic field
ρ :free stream density	β_C:coefficient of expansion with concentration
μ:fluid viscosity	β_T:coefficient of thermal expansion
$\bar{\mu}$:viscosity of porous media	C:concentration of the fluid inside the boundary
g:gravitational acceleration,	T :temperature inside the boundary layer
k:thermal conductivity,	C_b:second order inertial resistance
σ_m:electrical conductivity	D_m:coefficient of mass diffusivity
C_∞:ambient concentration	l:order of the chemical reaction
T_∞:ambient temperature	K_R:dimensional chemical reaction parameter